Diiron Bridged-Thiolate Complexes That Bind N_2 at the $Fe^{II}Fe^{II}$, $Fe^{II}Fe^{I}$, and $Fe^{I}Fe^{I}$ Redox States

Sidney E. Creutz and Jonas C. Peters*

Division of Chemistry and Chemical Engineering, California Institute of Technology, Pasadena, California 91125, United States

S *Supporting Information*

ABSTRACT: All known nitrogenase cofactors are rich in both sulfur and iron and are presumed capable of binding and reducing N_2. Nonetheless, synthetic examples of transition metal model complexes that bind N_2 and also feature sulfur donor ligands remain scarce. We report herein an unusual series of low-valent diiron complexes featuring thiolate and dinitrogen ligands. A new binucleating ligand scaffold is introduced that supports an $Fe(\mu$-SAr)Fe diiron subunit that coordinates dinitrogen (N_2-$Fe(\mu$-SAr)Fe-N_2) across at least three oxidation states ($Fe^{II}Fe^{II}$, $Fe^{II}Fe^{I}$, and $Fe^{I}Fe^{I}$). The (N_2-$Fe(\mu$-SAr)Fe-N_2) system undergoes reduction of the bound N_2 to produce NH_3 (~50% yield) and can efficiently catalyze the disproportionation of N_2H_4 to NH_3 and N_2. The present scaffold also supports dinitrogen binding concomitant with hydride as a co-ligand. Synthetic model complexes of these types are desirable to ultimately constrain hypotheses regarding Fe-mediated nitrogen fixation in synthetic and biological systems.

Although biological nitrogen fixation mediated by the iron–molybdenum cofactor (FeMoco) of MoFe-nitrogenase enzymes has inspired a wealth of synthetic model studies,[1−4] the modeling field is marked by a sharp dichotomy between functional and structural models of the FeMoco cluster. In the crystallographically characterized state of the biological Fe_7MoS_9 cluster, the "belt" irons that are hypothesized to be likely initial binding site(s) for N_2[5] are in an FeS_3C coordination environment consisting of three sulfides bridged to either one or two additional metal centers (Fe or Mo) and the interstitial carbide (C^{4-}) ligand (Figure 1).[6] In contrast, synthetic iron complexes for which spectroscopically and/or structurally characterized N_2 complexes are known are dominated by ligands composed primarily of phosphorus and nitrogen donors.

Sulfur-supported transition metal complexes that bind N_2 remain very uncommon.[8] This state of affairs is particularly noteworthy for iron, especially in the context of nitrogenase
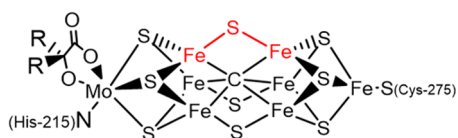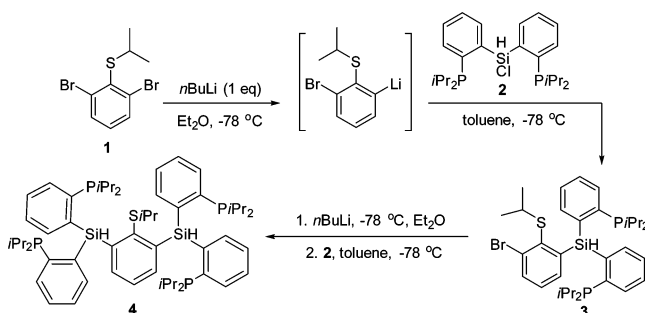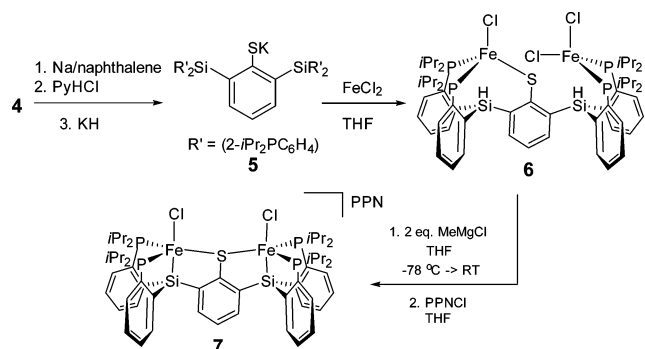
Scheme 1. Synthesis of Protected Ligand 4

Scheme 2. Synthesis of 6 and 7

model chemistry; reported examples of iron centers ligated to a sulfur donor ligand of any kind (e.g., S^{2-}, SR^-, SR_2) and at the same time an N_2 ligand are few in number, limited to several $Fe(N_2)(thioether)$ derivatives.[9] No examples of $Fe(N_2)$ complexes involving anionic sulfur donors (sulfides or thiolates) have ever been reported,[10] despite numerous examples of synthetic iron sulfide and iron thiolate complexes and clusters.[11] This is perhaps not surprising: sulfides and thiolates/thioethers typically act as weak-field ligands that do not give rise to the types of low-spin and low-valent iron centers that are well-suited to bind N_2.[8b,12] The few examples of low-valent, low-coordinate diiron bridged-sulfide complexes ($Fe(\mu$-S)Fe) that are known have not yet been observed to bind N_2.[12]

Herein we pursue a strategy to overcome these challenges via a binucleating ligand scaffold designed with a mixed phosphine–thiolate coordination environment that places iron in a trigonal

Figure 1. Representation of the nitrogenase iron–molybdenum cofactor, highlighting one candidate Fe–S–Fe substrate binding site.[7]
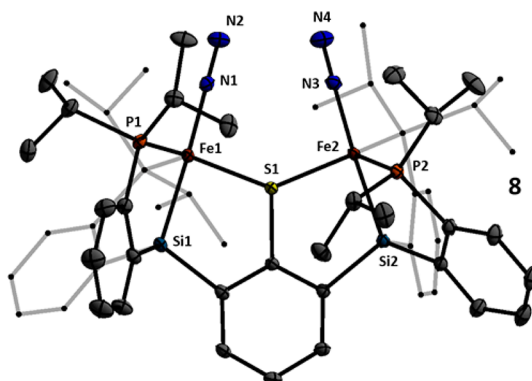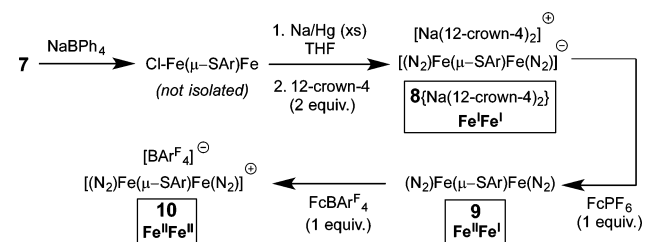
Scheme 3. Synthesis of Fe−N₂ Adducts {8}⁻, 9, and 10

Figure 2. Crystal structure of {8}{Na(12-crown-4)₂}. The counter-cation (Na(12-crown-4)₂), solvent molecules, and hydrogen atoms are omitted for clarity. Thermal ellipsoids shown at 50% probability.

geometry. This strategy affords a bridging Fe(μ-SAr)Fe moiety with high-affinity Fe−N₂ binding sites across three redox states.

The binucleating ligand of choice and its synthesis are shown in Schemes 1 and 2. Monolithiation of thioether **1** followed by reaction with chlorosilane electrophile **2** gives the diphosphine–thioether product **3**; a second lithiation and electrophile addition affords the protected ligand **4** in good yield. Deprotection of the isopropyl thioether with sodium naphthalenide provides the thiolate ligand **5** which, when stirred with 2 equiv of FeCl₂, generates a metalated brown paramagnetic solid product formulated as **6** (Scheme 2).

Treating **6** with 2 equiv of methyl Grignard followed by [PPN]Cl (PPN = bis(triphenylphosphine)iminium) results in formal loss of 2 equiv of methane and concomitant installation of the Fe−Si bonds to provide an anionic diiron(II) dichloride complex, **7**, as its PPN salt (Scheme 2). Complex **7** is a paramagnetic, bright red solid and has been crystallographically characterized (see SI); its structure shows two trigonal bipyramidal Fe−Cl sites within a bis(phosphine)silyl binding pocket (axial chloride *trans* to axial silyl) that are symmetrically bridged by the arylthiolate. The two SiP₂FeCl subunits are canted with respect to the central arene ring; the Cl−Fe−Fe−Cl dihedral angle is 36°.

Entry to the desired series of diiron N₂ adduct complexes was next pursued. Treatment of **7** with NaBPh₄ gives a putative intermediate monochloride complex (with loss of NaCl and [PPN][BPh₄]) which, when followed by reduction with excess sodium amalgam in THF, affords the anion {N₂-Fe^I(μ-SAr)Fe^I-N₂}⁻ (**8**) as a {Na(THF)$_x$}⁺ salt (Scheme 3). Treatment of this salt with 12-crown-4 sequesters the sodium countercation to give {N₂-Fe^I(μ-SAr)Fe^I-N₂}{Na(12-crown-4)₂} ({8}{Na(12-crown-4)₂}). The solid-state structure of {8}{Na(12-crown-4)₂} shows coordination of a terminally bound N₂ ligand at each of the two iron centers at the axial position *trans* to the silyl donor and *cis* to the bridging arylthiolate linker (Figure 2). Anion **8** displays two
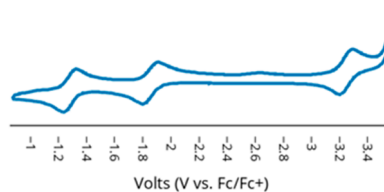

Figure 3. CV of **9**, measured in 0.4 M [TBA][PF₆] in THF at 100 mV/s and internally referenced to Fc/Fc⁺.

Table 1. Comparison of Selected Bond Lengths and Spectroscopic Parameters for Complexes 8−12

	Fe−P (Å, avg)	Fe−S (Å, avg)	Fe−S−Fe (deg)	ν(NN) (cm⁻¹)
8	2.226	2.184	137.098(15)	2017, 1979
9	2.291	2.208	135.52(5)	2070, 1983
10	2.341	2.244	138.02(4)	2129
11	2.264	2.189	136.562(15)	2036, 2093
12	2.219	2.332	140.42(3)	2044, 1981

IR absorption features corresponding to the symmetric and asymmetric stretches arising from the two chemically equivalent N₂ ligands.[14] These shift from 1978 and 1928 cm⁻¹ in the ion-paired {Na(THF)$_x$}⁺ salt {8}{Na(THF)$_x$} (thin film deposited from THF) to 2017 and 1979 cm⁻¹ in {8}{Na(12-crown-4)₂}. Both salts of the formally diiron(I) anion **8** are deep green in color and diamagnetic due to strong coupling.

Stepwise oxidation of **8** with FcPF₆ followed by FcBAr^F₄ gives the mixed-valent N₂-Fe^II(μ-SAr)Fe^I-N₂ complex **9** and then the cationic {N₂-Fe^II(μ-SAr)Fe^II-N₂}⁺ complex **10**, respectively; both complexes have also been crystallographically characterized (Scheme 3; crystal structures are provided in the SI). Electrochemical characterization of mixed-valent **9** by cyclic voltammetry (CV, Figure 3) shows a reversible oxidation (generating **10**) at −1.3 V (vs Fc/Fc⁺) and reversible reductions at −1.9 and −3.3 V. The first reduction (−1.9 V) gives the anion **8**, while the second reduction apparently generates a more highly reduced, dianionic {N₂-Fe^I(μ-SAr)Fe^0-N₂}²⁻ species that has not been isolated.

Compounds **8**, **9**, and **10** have very similar overall solid-state structures despite minor changes in the bond lengths of the immediate iron coordination environment (Table 1), consistent with the reversible CV data described above. The Fe−P bond lengths within **8**−**10** show little variation, and the Fe−S bonds are nearly symmetrical; only average bond lengths are therefore shown in Table 1.

Studies on nitrogen reduction by FeMoco suggest that iron hydride species may play an important mechanistic role and access to EPR active models of such species can help to constrain spectroscopic parameters (e.g., EPR/ENDOR) for potential hydride intermediate assignments.[15,16] Synthetic access to N₂/hydride species within the present iron thiolate-N₂ model system proved viable. When complex **6** is reduced with excess sodium amalgam in benzene, a new hydride product, {(N₂)Fe^II(μ-SAr)Fe^II N₂(H)} (**11**), is produced cleanly (Scheme 4). Complex **11** is an orange-brown, diamagnetic solid featuring two uncoupled ³¹P NMR resonances in a 1:1 ratio at 84 and 94 ppm. The ¹H NMR spectrum of **11** shows a triplet at −13 ppm that integrates to a single hydride and is coupled only to the more downfield phosphorus resonance. These data allow the position of the hydride to be assigned as *trans* to the thiolate ligand between two phosphine ligands at one of the two iron centers. Additionally, the IR spectrum of **11** shows two sharp and strong
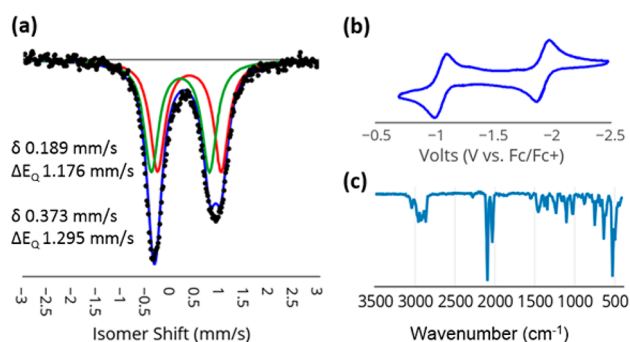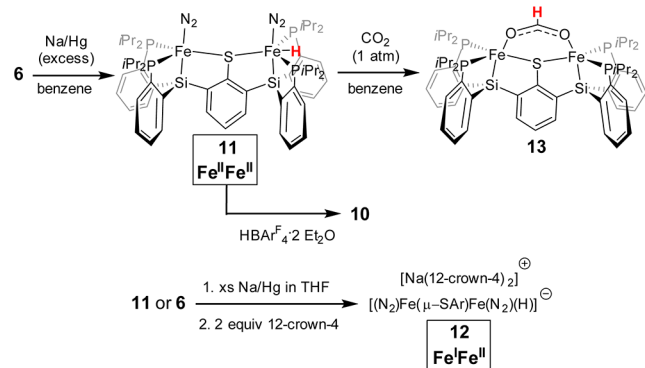
Scheme 4. Synthetic Access to Hydrides 11 and 12

Figure 4. Spectroscopic characterization of **11**. (a) Mossbauer spectrum of microcrystalline **11** (80 K, suspended in boron nitride matrix). Parameters for the displayed fit are shown. (b) CV measured in 0.4 M [TBA][PF_6] in THF at 100 mV/s and internally referenced to Fc/Fc$^+$. (c) IR spectrum of **11** as a thin film deposited from benzene solution.

peaks at 2036 and 2096 cm^{-1}, corresponding to two inequivalent N≡N stretches (Figure 4). The Mossbauer spectrum of **11** also indicates inequivalent iron centers with two quadrupole doublets in a 1:1 ratio. Complex **11** has been crystallographically characterized, but the hydride position could not be located from the data and, as the molecule sits on a crystallographically imposed 2-fold rotation axis (see SI), its position could not be indirectly inferred.

To chemically confirm the presence of the hydride ligand, **11** was exposed to an atmosphere of CO_2 in benzene. This reaction quantitatively affords the product of CO_2 insertion into the Fe–H bond (**13**, Scheme 4). Bright red, paramagnetic diiron(II) **13** has been crystallographically characterized (see SI), showing a bridged formate that is κ^1 with respect to each Fe center. The structure of **13** suggests that this diiron platform may be interesting to pursue in the context of bimetallic CO_2 reduction catalysis. Treatment of **11** with 1 equiv of HBAr$^F_4$·2Et$_2$O cleanly generates **10** via loss of H_2.

The CV of hydride **11** shows reversible oxidation (−1.1 V) and reduction (−2.0 V) events (Figure 4b). The anionic {(N_2)Fe^{II}(μ-SAr)FeN_2(H)}$^-$ reduction product, **12**, can be isolated and crystallographically characterized. This is achieved by stirring **11** (or **6**) over sodium amalgam in THF followed by treatment with 12-crown-4 (Scheme 4). Complex **12** is a paramagnetic brown solid with sharp, strong IR absorbance features at 2044 and 1981 cm^{-1} (shifted from 1999 and 1928 cm^{-1} prior to treatment with 12-crown-4). Its crystal structure (Figure 5) shows a wide P–Fe–P angle at Fe1 (147.72(4)°) compared to that at Fe2 (113.06(3)°). This variation reflects the presence of a hydride ligand at Fe1, apparently in a position *trans* to the bridged
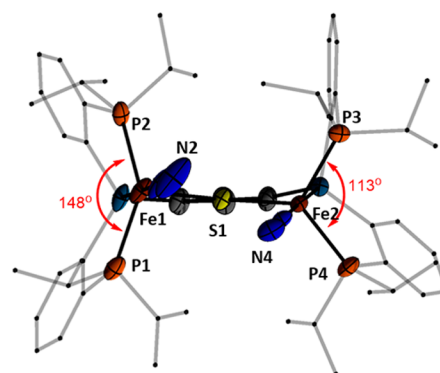

Figure 5. Crystal structure of **12** highlighting differing P–Fe–P angles due to the presence of a hydride ligand on Fe1 between P1 and P2. Countercation (Na(12-crown-4)$_2$), solvent molecules, and hydrogen atoms (including hydride, which was not crystallographically located) omitted for clarity; thermal ellipsoids shown at 50% probability.

Scheme 5. NH$_3$ Generation from N$_2$ or N$_2$H$_4$
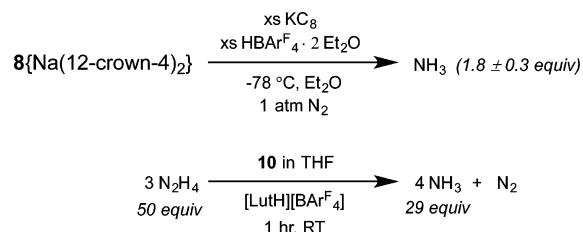
thiolate donor as assigned to the solution structure of diamagnetic **11**. By contrast to the solid-state structures of **8**–**10** that show symmetric or near-symmetric coordination of the bridged-thiolate ligand (Table 1), the two iron sites of **14** have distinct Fe–S bond lengths: an elongated Fe–S bond of 2.3744(7) Å to the hydride-bound Fe1 site and a shorter Fe–S bond of 2.2893(7) Å at the Fe2 site. The difference presumably reflects a *trans* influence from the hydride ligand at Fe1.

Biomimetic reactivity of the Fe-(μ-SAr)-Fe subunit in the present scaffold has been explored via the reduction or decomposition of the nitrogenase substrates N_2 and N_2H_4; in both these cases cleavage of the N–N bond has been demonstrated. For instance, treatment of **8**{Na(12-crown-4)$_2$} with an excess (100 equiv) of KC$_8$ and HBAr$^F_4$·2Et$_2$O in the presence of an N_2 atmosphere (Et$_2$O, −78 °C, 2 h) produces 1.8 ± 0.3 equiv of ammonia (NH$_3$); this yield is comparable to that achieved by the related monometallic silyl-anchored iron complex, {[SiP$^{iPr}_3$]FeN_2}{Na(12-crown-4)$_2$} (Scheme 5).[17] The comparatively low yield of NH$_3$ production from **8**{Na-(12-crown-4)$_2$} may reflect rapid generation of H_2 instead. No NH$_3$ is produced when **8**{Na(12-crown-4)$_2$} is treated with acid in the absence of added reductant.

By contrast to its modest N_2-reducing capacity, the cationic complex **10** serves as an effective precatalyst for hydrazine disproportionation to NH$_3$ and N_2 with a turnover number (TON) that is significantly higher than previously reported for any iron complex.[18] Reproducible yields of NH$_3$ were only achieved in the presence of an acid co-catalyst (Scheme 5). Thus, treatment of **10** in THF with 1 equiv of [LutH][BAr$^F_4$] and 50 equiv of N_2H_4 produced 29 equiv of NH$_3$ during the course of 1 h at room temperature (LutH = lutidinium). The TON appears to be limited by catalyst decomposition; neither longer reaction times nor higher concentrations of N_2H_4 resulted in higher yields

of NH_3. For comparison, a related monometallic iron complex of a silyl-anchored bisphosphine thioether ligand, $\{[SiP^{iPr}_2S^{Ad}]^-FeN_2\}\{BAr^F_4\}$,[9b] produced <2 equiv of NH_3 under the same reaction conditions, even with longer reaction times (8 h); this comparison suggests the possibility that some degree of bimetallic cooperativity and/or the presence of the bridging thiolate as a proton shuttle may be important in facilitating the N−N bond cleavage of hydrazines catalyzed by **10**. Mechanistic studies will be interesting in this context since hydrazine has been suggested as a possible intermediate in dinitrogen reduction where the N−N bond is cleaved at a late stage; it can be converted to NH_3 either by further reduction or by a disproportionation pathway that also produces N_2.[19]

To conclude, a paradox in inorganic synthesis is the dichotomy between the sulfur-rich coordination environment of the iron and molybdenum centers of the FeMoco, and the dearth of well-defined N_2 adducts for these metals (and all transition metals) featuring sulfur donor ligands.[20] The synthetic work described here has provided the first examples[10] of thiolate-ligated Fe−N_2 species via a bimetallic Fe-(μ-SAr)-Fe subunit benefiting from a combination of phosphine and silyl donors. This subunit moreover shows that the N_2 ligands are retained across at least three redox states ($Fe^{II}Fe^{II}$, $Fe^{II}Fe^{I}$, $Fe^{I}Fe^{I}$) in the presence of the thiolate donor. This is significant because formally low-valent iron sites in the presence of S^{2-} or SH^- are plausible intermediates of biological nitrogen fixation but are not well represented in the synthetic literature. Synthetic access to terminally bonded iron hydrides in the presence of the bridging thiolate and N_2 ligands has also been established.[21] Finally, the ability of the present scaffold to mediate the stoichiometric and catalytic cleavage of N−N bonds has been briefly explored. Ongoing work will further examine the reactivity patterns of these (N_2)Fe-(μ-SAr)-Fe(N_2) subunits in the context of nitrogen fixation and reduction catalysis (e.g., H$^+$, CO_2) more generally.

■ ASSOCIATED CONTENT

ⓈSupporting Information

Synthetic and spectroscopic details for new compounds; crystal structures of **7**, **9−11**, and **13**; details of NH_3 production experiments. The Supporting Information is available free of charge on the ACS Publications website at DOI: 10.1021/jacs.5b04738.

■ AUTHOR INFORMATION

Corresponding Author

*jpeters@caltech.edu

Notes

The authors declare no competing financial interest.

■ ACKNOWLEDGMENTS

■ REFERENCES

(1) (a) MacKay, B. A.; Fryzuk, M. D. *Chem. Rev.* **2004**, *104*, 385. (b) Peters, J. C.; Mehn, M. P. In *Activation of Small Molecules*; Tolman, W. B., Ed.; Wiley-VCH: Weinheim, 2006; p 81.

(2) MacLeod, K. C.; Holland, P. L. *Nat. Chem.* **2013**, *5*, 559.

(3) Crossland, J. L.; Tyler, D. R. *Coord. Chem. Rev.* **2010**, *254*, 1883.

(4) Barrière, F. In *Biosinspired Catalysis: Metal-Sulfur Complexes*; Wiley: Weinheim, 2015; Chap. 9.

(5) Lukoyanov, D.; Dikanov, S. A.; Yang, Z.-Y.; Barney, B. M.; Samoilova, R. I.; Narasimhulu, K. V.; Dean, D. R.; Seefeldt, L. C.; Hoffman, B. M. *J. Am. Chem. Soc.* **2011**, *133*, 11655.

(6) (a) Einsle, O.; Tezcan, A.; Andrade, S. L. A.; Schmid, B.; Yoshida, M.; Howard, J. B.; Rees, D. C. *Science* **2002**, *297*, 1696. (b) Spatzal, T.; Aksoyoglu, M.; Zhang, L.; Andrade, S. L. A.; Schleicher, E.; Weber, S.; Rees, D. C.; Einsle, O. *Science* **2011**, *334*, 940. (c) Lancaster, K. M.; Roemelt, M.; Ettenhuber, P.; Hu, Y.; Ribbe, M. W.; Neese, F.; Bergmann, U.; DeBeer, S. *Science* **2011**, *334*, 974. (d) Lancaster, K. M.; Hu, Y.; Bergmann, U.; Ribbe, M. W.; DeBeer, S. *J. Am. Chem. Soc.* **2013**, *135*, 610. (e) Wiig, J. A.; Hu, Y.; Lee, C. C.; Ribbe, M. W. *Science* **2012**, *337*, 1672.

(7) (a) Lee, H. I.; Igarashi, R. Y.; Laryukhin, M.; Doan, P. E.; Dos Santos, P. C.; Dean, D. R.; Seefeldt, L. C.; Hoffman, B. M. *J. Am. Chem. Soc.* **2004**, *126*, 9563. (b) Spatzal, T.; Perez, K. A.; Einsle, O.; Howard, J. B.; Rees, D. C. *Science* **2014**, *345*, 1620.

(8) (a) Yoshida, T.; Adachi, T.; Kaminaka, M.; Ueda, T.; Higuchi, T. *J. Am. Chem. Soc.* **1988**, *110*, 4872. (b) Pombeiro, A. J. L.; Hitchcock, P. B.; Richards, R. L. *J. Chem. Soc., Dalton Trans.* **1987**, 319. (c) Cruz-Garritz, D.; Torrens, H.; Leal, J.; Richards, R. L. *Transition Met. Chem.* **1983**, *8*, 127. (d) Morris, R. H.; Ressner, J. M.; Sawyer, J. F.; Shiralian, M. *J. Am. Chem. Soc.* **1984**, *106*, 3683. (e) Dilworth, J. R.; Hu, J.; Thompson, R. M.; Hughes, D. L. *Chem. Commun.* **1992**, 551. (f) Seymore, S. B.; Brown, S. N. *Inorg. Chem.* **2006**, *45*, 9540. (g) Mori, H.; Seino, H.; Hidai, M.; Mizobe, Y. *Angew. Chem., Int. Ed.* **2007**, *46*, 5431. (h) Sellmann, D.; Hautsch, B.; Rosler, A.; Heinemann, F. W. *Angew. Chem., Int. Ed.* **2001**, *40*, 1505. (i) Sellmann, D.; Hille, A.; Rosler, A.; Heinemann, F. W.; Moll, M. *Inorg. Chim. Acta* **2004**, *357*, 3336. (j) Fernandez, P.; Sousa-Pedrares, A.; Romero, J.; Duran, M. L.; Sousa, A.; Perez-Lourido, P.; Garcia-Vazquez, J. A. *Eur. J. Inorg. Chem.* **2010**, 814.

(9) (a) Bart, S.; Lobkovsky, E.; Bill, E.; Wieghardt, K.; Chirik, P. J. *Inorg. Chem.* **2007**, *46*, 7055. (b) Takaoka, A.; Mankad, N. P.; Peters, J. C. *J. Am. Chem. Soc.* **2011**, *133*, 8440.

(10) We are aware of recent work from the Holland group at Yale, where an Fe−N_2 complex that features both thiolate and arene donors has been characterized (with permission; personal communication).

(11) (a) Lee, S. C.; Lo, W.; Holm, R. H. *Chem. Rev.* **2014**, *114*, 3579. (b) Rao, P. V.; Holm, R. H. *Chem. Rev.* **2004**, *104*, 527. (c) Malinak, S. M.; Coucouvanis, D. *Prog. Inorg. Chem.* **2001**, *49*, 599.

(12) (a) Lane, R. W.; Ibers, J. A.; Frankel, R. B.; Papaeftymiou, G. C.; Holm, R. H. *J. Am. Chem. Soc.* **1977**, *99*, 84. (b) Lee, S. C.; Holm, R. H. *Chem. Rev.* **2004**, *104*, 1135. (c) Malianak, S. M.; Coucouvanis, D. *Prog. Inorg. Chem.* **2001**, *49*, 599.

(13) (a) Anderson, J. S.; Peters, J. C. *Angew. Chem., Int. Ed.* **2014**, *53*, 5978. (b) Rodriguez, M. M.; Stubbert, B. D.; Scarborough, C. C.; Brennessel, W. W.; Bill, E.; Holland, P. L. *Angew. Chem., Int. Ed.* **2012**, *51*, 8247.

(14) Rittle, J.; McCrory, C.; Peters, J. C. *J. Am. Chem. Soc.* **2014**, *136*, 13853.

(15) (a) Hoffman, B. M.; Lukoyanov, D.; Yang, Z.-Y.; Dean, D. R.; Seefeldt, L. C. *Chem. Rev.* **2014**, *114*, 4041. (b) Hoffman, B. M.; Dean, D. R.; Seefeldt, L. C. *Acc. Chem. Res.* **2009**, *42*, 609.

(16) Kinney, R. A.; Saouma, C. T.; Peters, J. C.; Hoffman, B. M. *J. Am. Chem. Soc.* **2012**, *134*, 12637.

(17) Anderson, J. S.; Rittle, J.; Peters, J. C. *Nature* **2013**, *501*, 84.

(18) (a) Chen, Y.; Zhou, Y.; Chen, P.; Tao, Y.; Li, Y.; Qu, J. *J. Am. Chem. Soc.* **2008**, *130*, 15250. (b) Chang, Y.-H.; Chan, P.-M.; Tsai, Y.-F.; Lee, G.-H.; Hsu, H.-F. *Inorg. Chem.* **2014**, *53*, 664. (c) Umehara, K.; Kuwata, S.; Ikariya, T. *J. Am. Chem. Soc.* **2013**, *135*, 6754.

(19) Davis, L. C. *Arch. Biochem. Biophys.* **1980**, *204*, 270.

(20) Sellmann, D.; Sutter, J. *Acc. Chem. Res.* **1997**, *30*, 460.

(21) Diiron thiolate-bridged iron hydrides are also structurally relevant to hydrogenases. See, for example: Wang, W.; Rauchfuss, T. B.; Zhu, L. *J. Am. Chem. Soc.* **2014**, *136*, 5773.